RSC Advances

PAPER

View Article Online
View Journal | View Issue

Cite this: *RSC Adv.*, 2015, **5**, 937

Mass-analyzed-threshold-ionization (MATI) spectroscopy of 1,2,3-substituted halogenated benzenes *via* different intermediate vibrational states in the S_1 state

Sascha Krüger, Frank Witte, Jan Helfrich and Jürgen Grotemeyer*

For the first time, two color resonant mass analyzed threshold ionization (MATI) spectroscopy has been applied in order to investigate the ionic properties of 1,3-dichloro-2-fluoro-benzene (1,3,2-DCFB) and 1,3-difluoro-2-chloro-benzene (1,3,2-DFCB) radical cations in their electronic ground state. The ionic ground state of the different samples has been investigated *via* different S_1 intermediate states and compared to 1,2,3-trichlorobenzene measured in previous work. Additionally quantum chemical calculations at DFT (density functional theory) and TDDFT (time-dependent density functional theory) level of theory have been performed to support experimental findings. From the MATI spectra the adiabatic ionization energies of 1,3-dichloro-2-fluorobenzene and 1,3-fluoro-2-chlorobenzene could be determined to be 75.242 ± 6 cm^{-1} and 75.627 ± 6 cm^{-1}, respectively. Several vibrational modes of both compounds have been assigned by comparison of the experimental and theoretical results.

Received 21st October 2014
Accepted 24th November 2014

DOI: 10.1039/c4ra12873g

www.rsc.org/advances

1. Introduction

Halogenated aromatic molecules became a topic of great interest due to their widespread presence in industrial processes and hence presence in the environment as potentially toxic and cancerogenic pollutants. Moreover halogenated benzenes are important model substances to validate theoretical concepts, such as vibronic coupling and others. As one of the spectroscopically best-investigated molecules of all, benzene can serve as an outstanding reference system to study the influence of tailored perturbations, such as careful choice of substitution pattern, to the (ro)vibronic structure. As an immediate effect a shift in transition energies, ionization energy, molecular geometry and vibrational frequencies can be observed. The characteristics of these effects strongly depend on the number, type and localization of the substituents. As the magnitude of these effects are rather small (from a few wavenumbers up to a hundred wavenumbers), high resolution techniques, such as mass analyzed threshold ionization (MATI) or zero kinetic energy (ZEKE) spectroscopy are ideally suited to investigate such phenomena.[1–4] Chloro- and fluoro-benzenes have been subject to various studies investigating the vibronic properties of the first electronic excited state (S_1) as well as cationic ground state (D_0).[1,5–13] In this paper we will focus particularly on out-of-plane b_1-symmetric modes. Modes of this symmetry are connected to interesting phenomena observed in a whole variety of halobenzenes. For example, difluorobenzenes exhibit large frequency lowering of b_1 (b_{3u} under D_{2h} in case of *p*-DFB) symmetric modes in going from S_0 to S_1 or from D_0 to S_1,[14] respectively. The intensity gain of this symmetry forbidden mode was interpreted in terms of the pseudo-Jahn–Teller effect (PJTE). The PJTE is based on the idea that a geometrical distortion blurs the difference in symmetry between two or more electronic states of virtually equal energy. In 1,2,4,5-tetrafluorobenzene (D_{2h}) it was found that the b_{2g}-symmetric mode 11 shows an unusual strong activity in the form of a long progression (ν_{11}^{2n}). Recent results show that the planarity of this molecule is distorted along the eigenvector of the 11 mode during excitation to $^1B_{2u}S_1$ state. It is an interesting question to elucidate if these phenomena can be extended to further congeners and identified as a general feature. In particular in the case of the molecular geometry change it is crucial to determine the involved vibrational modes and participating electronic states. For this purpose, the experimental data are compared to theoretical calculations, which enable the possibility of assigning the observed vibrational modes. In this paper we present mass-selected two color two photon Resonance Enhanced Multi Photon Ionization (2C2P-REMPI) spectra of the $S_1 \leftarrow S_0$ transition and MATI spectra *via* different S_1-intermediate states of 1,3-dichloro-2-fluorobenzene and 1,3-dichloro-2-fluorobenzene. Some assignments of 1,2,3-trichlorobenzene reported previously[1] were reconsidered and compared to the newly gained knowledge.

Institut für Physikalische Chemie, Christian-Albrechts-Universität Kiel, Max-Eyth Str. 1, 24118 Kiel, Germany. E-mail: grote@phc.uni-kiel.de

2. Experimental setup

The experimental setup consists of a homemade time-of-flight (TOF) mass spectrometer as described in detail previously.[1,15,16] Briefly, the spectrometer consists of a standard second order corrected reflectron time-of-flight mass spectrometer equipped with single stage ion source. The laser system used for excitation and ionization consists of two dye lasers (Laser Analytical Systems LDL 205, Lambda Physics FL 3002). Each dye laser is pumped by a dedicated Nd:YAG laser (Lumonics HY-1200, Continuum Surelite II). A Quantum Composers 9600+ delay pulse generator fed by an external clock operated at 10 Hz controls flash lamp and Q-switch delays. The output of each dye laser is frequency-doubled by a BBO-I crystal yielding tunable ranges from 245 to 285 nm. Wavelength calibration of both dye lasers is performed by recording an optogalvanic spectrum with a neon hollow cathode lamp yielding accuracy better than 2 cm^{-1}. Initially a supersonic molecular beam of sample molecules and seed gas (argon) with a backing pressure of approximately 2 bar is expanded *via* a pulsed jet valve (General Valves Series 9) into the ion source. To obtain a sufficient vapor pressure the sample is heated to approximately 80 °C. Excitation or ionization is accomplished by multi photon absorption under field-free conditions. In the MATI modus, promptly generated ions are discriminated against Rydberg neutrals through the application of a weak electrical field of 1–2 V cm^{-1} by a subsequent delay (~100 ns) to multi-photon excitation. Finally, a high voltage pulse (890 V cm^{-1}) switched by a Behlke HS56-01 fast thyristor ionizes the Rydberg neutrals and accelerates them into the mass spectrometer. In REMPI modus, the generated ions are accelerated directly into the TOF without the retarding field. The ion signal is detected by a conventional dual micro-channel-plate detector and transferred to a LeCroy 534M digital oscilloscope. A computer, linked to the oscilloscope by a GPIB connection performs the data acquisition and processing. The 123-DCFB was purchased from Aldrich, 126-DFCB from ABCR and were used without further purification.

3. Quantum-chemical calculations

Quantum chemical calculations were performed in order to assign the observed vibrational bands and to support the experimental findings. The software package Turbomole[17–20] was used for all quantum chemical calculations. Geometry optimizations and subsequent frequency analyses for molecules in the electronic ground state (S_0) and the cationic ground state (D_0) were conducted at the density functional theory (DFT) level of theory with both the gradient corrected functional BP86 [21a] and the hybrid functional B3LYP.[21b] The triple basis set TZVPP[21c] has been applied to all DFT calculations. Calculations for the S_1 were done analogously using the time dependent density functional theory (TDDFT). For comparison reasons, geometry calculations and frequency analyses were also treated at the coupled cluster (CC2) level of theory for the S_0- and S_1-state using the Ahlrichs basis set cc-pVTZ.[21d] The nomenclature used for assignment of vibrational bands is according to Varsanyi and Szoke,[22] which is derived from Wilson's notation of the Benzene modes.[23]

We refrained from the use of scaling factors to fit the calculated frequencies.

4. Experimental results

4.1. 1,3-Dichloro-2-fluorobenzene (1,3,2-DCFB)

4.1.1. REMPI spectrum. According to electric dipole selection rules the transition to first excited singlet state $^1B_2S_1(\pi^* \leftarrow \pi)$ in 1,3,2-DCFB is allowed (*y*-polarized). For benzene, the corresponding transition $A^1B_{2u} \leftarrow X^1A_{1g}$ is dipole forbidden under D_{6h} symmetry. The reduced symmetry in 1,3,2-DCFB (C_{2v}) leads to an electronically as well as vibronically allowed transition. Starting from the premise that the molecules are sufficiently cooled with regards to their degrees of freedom, only total symmetric (a_1) vibrations are allowed according to the Franck–Condon (FC) principle. Due to vibronic coupling to intensive, nearby states, vibrations of a_2 and b_2 symmetry can gain intensity as well. The REMPI spectrum shown in Fig. 1 in units of internal energy could be recorded in the range up to 1300 cm^{-1}. The excitation energy of the first excited state S_1 could be determined for the first time to be 36 460 ± 2 cm^{-1}.

Normal coordinate analysis for 1,3,2-DCFB yields following distribution of fundamental modes under C_{2v} symmetry: $\Gamma_{vib} = 11 \times a_1, 10 \times b_2, 3 \times a_2, 6 \times b_1$. Clearly, the spectrum is dominated by the total symmetric modes 1^1 (565 cm^{-1}) and 18a (977 cm^{-1}). Moreover the a_1-symmetric modes $9a^1$, $6a^1$, $7a^1$, 12^1 (186 cm^{-1}, 349 cm^{-1}, 792 cm^{-1}, 1104 cm^{-1}) could be identified with lower intensity. With $16a^1$ (360 cm^{-1}) also an a_2-symmetric mode could be assigned. As expected, no modes of b_1-symmetry could be assigned to the spectrum in accordance with selection rules. Particular attention should be paid to the low frequency band at 120 cm^{-1}. A band with such a low frequency can with certainty be assigned to an out-of-plain mode. Based on correlation with MATI spectra we assigned the first even overtone of the b_1-symmetric mode 17b to this band. The frequency of 52 cm^{-1} calculated with the coupled cluster method is in reasonable agreement with the experimental value for the half of the overtone for $17b^2$. The bands at 247 cm^{-1} (15^1), 337 cm^{-1} ($6b^1$), 500 cm^{-1} (3^1) and 1236 cm^{-1} ($18b^1$) were assigned to b_2-symmetric modes. The latter two experimental values are in excellent agreement with both calculated values (TDDFT, CC2) for the first excited singlet state of 1,2,3-DCFB. Comparing the calculated values for the 15^1 and $6b^1$ mode a major deviation becomes apparent, just like in the case of 17b. All performed calculations show good agreement with the experiment for the modes $9a^1$, $6a^1$, 1^1, $7a^1$, $18a^1$, 12^1, $16a^1$, whereas the best results were obtained with the CC2 level of theory (see Table 1).

4.1.2. MATI spectra. The MATI spectra *via* the S_1 intermediate states 0^0, $17b^1$, $9a^1$, 1^1 are shown in Fig. 2. The origin of the $D_0(^2B_1)$ state and with that the adiabatic ionization energy was found to be 75.242 ± 6 cm^{-1} (9.3288 ± 0.0007 eV). This value is in good accordance with the previously by conventional photoelectron spectroscopy determined value of 9.32 ± 0.02 eV.[25]

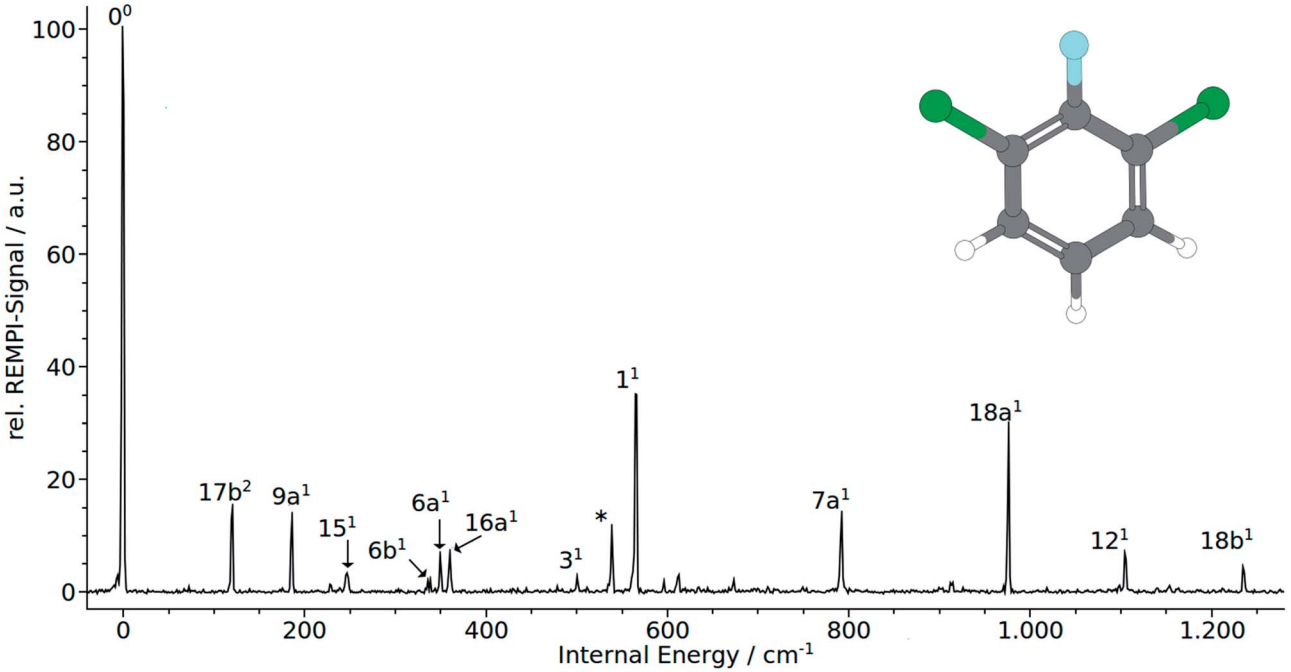

Fig. 1 (1 + 1′) REMPI spectrum of 1,3-dichloro-2-fluoro-benzene (1,3,2-DCFB).

Table 1 Comparison experimental and calculated normal modes observed in the S_0, S_1 and D_0 state of 1,3,2 DCFB

$S_0(C_{2v})$						S_1	(C_{2v})	(C_{2v})	(C_S)	D_0	(C_{2v})	
Wilson	Sym.	exp.	B3LYP	BP86	CC2	exp.	B3LYP	BP86	CC2	exp.	B3LYP	BP86
9a	a_1	256[a]	192	186	189	186	241	232	183	190	195	189
6a	a_1	376[a]	379	369	380	349	355	361	343	361	381	372
1	a_1	597[a]	601	584	596	565	538	522	558	578	603	586
7a	a_1	803[a]	839	813	829	792	831	815	791	798	820	797
18a	a_1	1058[a]	1092	1061	1080	977	1013	998	991		1047	1027
12	a_1	1112[a]	1116	1083	1124	1104	1077	1046	1079		1143	1104
13	a_1	1205[a]	1277	1240	1277		1314	1320	1242		1339	1295
19a	a_1	1462[a]	1490	1444	1485		1213	1229	1383		1459	1412
8a	a_1	1572[a]	1613	1564	1608		1509	1476	1512		1618	1567
20a	a_1	3084[a]	3189	3119	3220		3159	3080	3210		3197	3126
2	a_1		3212	3142	3243		3220	3147	3246		3218	3147
10a	a_2	215[a,b]	208	201	207		120	123	71	174	180	173
16a	a_2	530[a,b]	553	534	518	360	458	495	313	512	498	476
17a	a_2	894[a]	921	876	890		1045	1060	616		936	897
17b	b_1	115[a,b]	107	103	107	60[c]	31	38	52	95	88	85
10b	b_1	260[a,b]	282	271	278	270[c]	263	259	178	264	274	265
16b	b_1	513[a]	533	512	542		502	454	364	452	455	441
4	b_1	705[a]	732	699	680		766	755	460	732	743	715
11	b_1	770[a]	794	758	771		847	827	601	678	826	792
5	b_1	965[a]	983	937	949		1004	966	782		1009	966
15	b_2	279[a]	258	248	252	247	62	61	227	242	233	253
6b	b_2	401[a]	404	393	401	337	202	209	319	331	300	331
3	b_2	539[a]	545	528	538	500	500	498	519	471	513	504
7b	b_2	829[a]	798	779	810		698	683	759	827	812	796
9b	b_2	1154[a]	1180	1145	1170		1177	1144	1105		1083	1104
18b	b_2	1205[a,b]	1233	1193	1223	1236	1250	1185	1170		1330	1192
14	b_2	1255[a]	1313	1322	1421		1413	1360	1497		1226	1296
19b	b_2	1446[a]	1481	1432	1465		1446	1407	1389		1514	1466
8b	b_2	1583[a]	1615	1566	1608		1574	1545	1683		1371	1384
20b	b_2	3084[a]	3207	3137	3235		3188	3177	3141		3215	3144

[a] IR-band.[24] [b] From combination band. [c] From overtone.

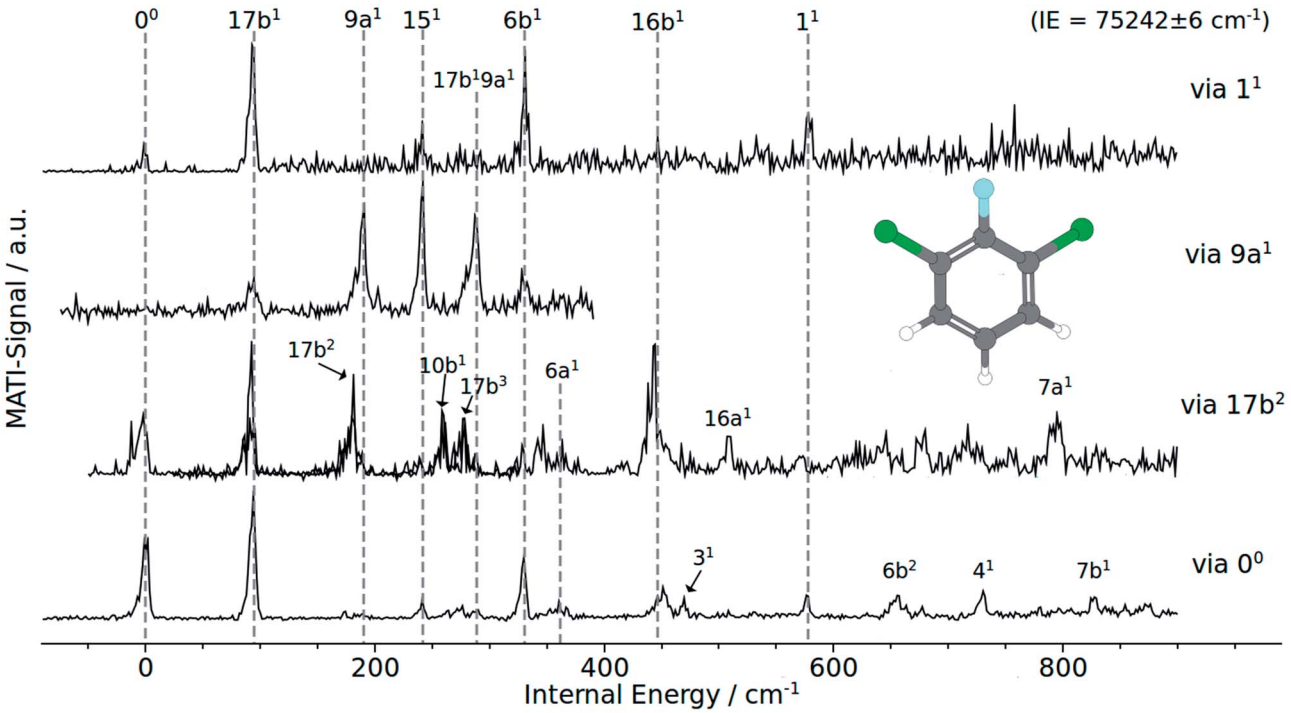

Fig. 2 MATI spectra of 1,3,2-DCFB of different vibrational intermediate states of the first excited electronic state: (a) *via* 1^1, (b) *via* $9a^1$, (c) *via* $17b^2$, (d) *via* the electronic origin (0^0).

Besides the 0^0 transition, the MATI spectrum obtained *via* the electronic origin exhibits several more additional resonances. The most prominent peak in the spectrum is the band assigned to the 17b mode, which is constituting a violation of the $\Delta v = 0$ propensity rule. Additionally, the mode $17b^1$ at 95 cm^{-1} appears as a combination band ($17b^19a^1$) at 288 cm^{-1}. Moreover the spectrum is conspicuously rich in b_1-symmetric modes. In addition to $17b^1$ we assigned the $10b^1$ (264 cm^{-1}), $16b^1$ (452 cm^{-1}), 11^1 (678 cm^{-1}) and 4^1 (732 cm^{-1}). Another out-of-plane vibration ($10a^1$) with a_2-symmetry and low intensity has been assigned to the band at 174 cm^{-1}. The bands at 361 cm^{-1}, 578 cm^{-1} have been assigned to the total symmetric modes $6a^1$ and 1^1, respectively. b_2 symmetric modes were identified at 242 cm^{-1} (15^1), 331 cm^{-1} ($6b^1$), 471 cm^{-1} (3^1) and 827 cm^{-1} ($7b^1$). The band at 657 cm^{-1} fits the overtone $6b^1$.

The MATI spectrum obtained *via* the S_117b^2 shows a short, three-membered regular progression with transitions corresponding to the excitation of one, two and three quanta. In contradiction to the $\Delta v = 0$ propensity rule, the band labeled $17b^1$ is the most prominent peak in the spectrum. It is notable that the 17b mode also appears in the combination bands $17b^19a^1$ (288 cm^{-1}) and $16b^16b^1$ (423 cm^{-1}). Also apparent is the richness in b_1-symmetric modes, first and foremost the intense $16b^1$ (448 cm^{-1}), but also the $10b^1$ (264 cm^{-1}), 11^1 (680 cm^{-1}), 4^1 (728 cm^{-1}). The MATI spectrum obtained *via* the S_19a^1 mode also shows a breakdown of the $\Delta v = 0$ propensity rule. Not the vertical transition into the D_09a^1 state is the dominating one, but the band at 242 cm^{-1} (15^1). In addition the 17b mode appears again, also as a combination in $17b^19a^1$. A further band at 331 cm^{-1} could be identified with $6b^1$. The measured values are in good accordance with the calculated values (195 and 189 cm^{-1} for the $9a^1$, 233 and 253 cm^{-1} for the15^1 and also 300 and 331 cm^{-1} for the $6b^1$).

The MATI spectrum *via* S_11^1 continues the series of MATI spectra characterized by a breakdown of the $\Delta v = 0$ propensity rule in favor for the vibronic transition into the D_017b^1 state. Further active modes that could be assigned in the recorded range up to 750 cm^{-1} are the 15^1 (241 cm^{-1}), $6b^1$ (331 cm^{-1}) and 1^1 (578 cm^{-1}). The experimentally determined frequency for the 1^1 mode is in good accordance with the calculated values of 578 cm^{-1} or 603 cm^{-1} respectively. It should be noticed that, owing to the heavy substituents, the displacement pattern of the 'ring-breathing-mode' shows a striking deviation from the original benzene pattern. It resembles clearly the pattern of mode 6a found for benzene. The assignment of the band at 578 cm^{-1} to the mode 6a is excluded since it was already doubtlessly assigned to the band at 361 cm^{-1}.

4.2. 1,3-Difluoro-2-chloro-benzene (1,3,2-DFCB)

4.2.1. REMPI spectrum. 1,3,2-DFCB belongs to C_{2v} point group and has a dipole allowed transition to the $^1A_1S_1(\pi^* \leftarrow \pi)$ first excited state. According to FC-principle only transitions in total symmetric (a_1) modes are allowed, b_1 and b_2 can gain intensity due to vibronic coupling mechanism, a_2 modes are symmetry forbidden. The REMPI spectrum shown in Fig. 3 in units of internal energy could be recorded in the range up to 800 cm^{-1}. The excitation energy of the first excited state S_1 could be determined for the first time to be 37 449 ± 2 cm^{-1}.

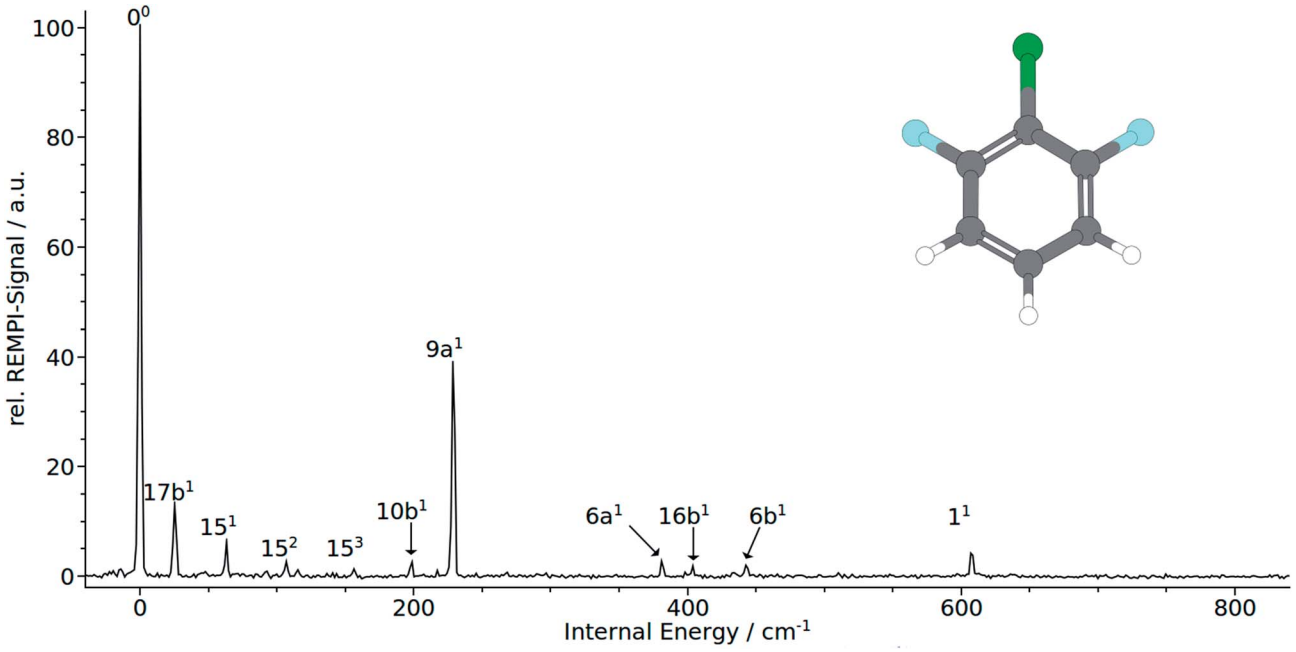

Fig. 3 (1 + 1′) REMPI spectrum of 1,3-difluoro-2-chloro-benzene (1,3,2-DFCB).

The electronic origin and the total symmetric mode $9a^1$ at 228 cm^{-1} dominates clearly the measured REMPI spectrum. It should be noted that the remaining bands at 381 cm^{-1} and 607 cm^{-1} that were both assigned to the total symmetric modes 6^1 and 1^1, respectively. Quite unusual for total symmetric modes we found poor consistency between calculated and observed bands: calculation substantially underestimate the $6a^1$ and 1^1 with 188 cm^{-1} to 202 cm^{-1} and 488 cm^{-1} to 517 cm^{-1}, respectively. The $9a^1$ has been overestimated with 364 cm^{-1} to 374 cm^{-1}. Nevertheless the correlation with MATI spectra backups the assignment of the total symmetric modes. Moreover, the calculations suggest the mode $7a^1$, that cannot be seen in the spectrum, to appear in the spectrum between 710 cm^{-1} and 750 cm^{-1}. As expected, no modes of a_2 symmetry could be assigned to the spectrum in accordance with selection rules. In contrast to 1,2,3-TCB and 1,3,2-DCFB, transitions to b_1-symmetric modes are allowed in 1,3,2-DFCB. The bands at 25, 98 and 404 cm^{-1} could be identified with the b_1-symmetric modes $17b^1$, $10b^1$ and $16b^1$. In this case, the calculated frequencies are in good agreement with the observed ones. The

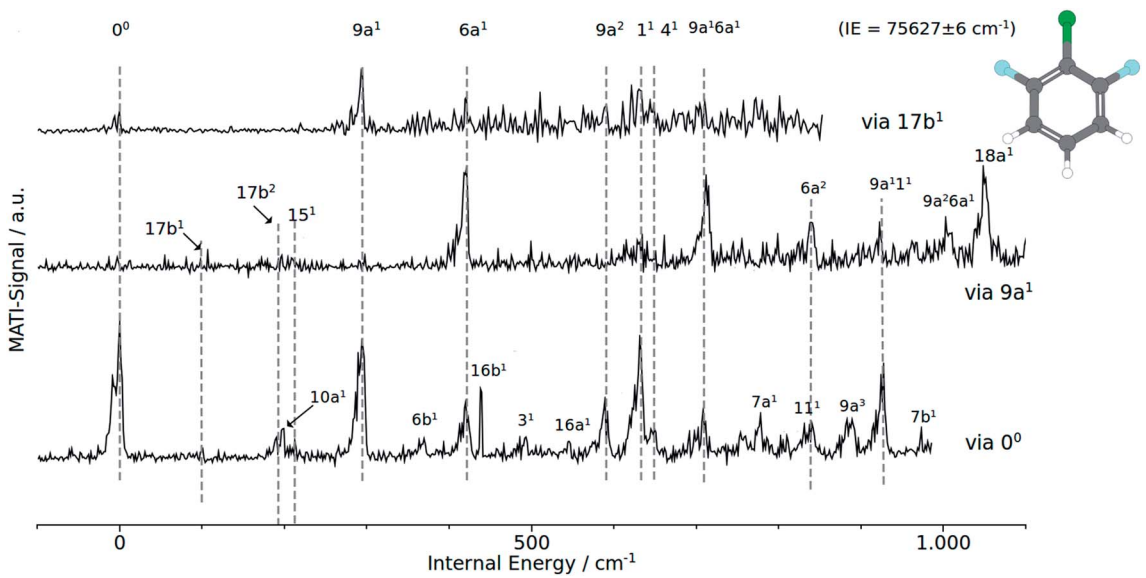

Fig. 4 MATI spectra of 1,2,6 DCFB of different vibrational intermediate states of the first excited electronic state: (a) *via* $9a^1$, (b) *via* $17b^2$, (c) *via* the electronic origin (0^0).

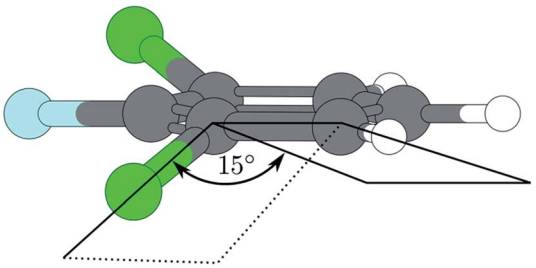

Fig. 5 Excited state geometry of 1,3,2-DCFB obtained by CC2-optimization.

17b^1 has been predicted to appear between 31 cm^{-1} and 51 cm^{-1}, the 10b^1 between 176 cm^{-1} and 215 cm^{-1} and the 16b^1 between 351 cm^{-1} and 428 cm^{-1}. With 15^1 and 6b^1 two a_2-symmetric modes could be assigned. Noteworthy is the appearance of the 15 mode as a short, three-membered progression of overtones (15^1, 15^2, 15^3). The measured frequencies of 443 cm^{-1} for 6b^1 and 63 cm^{-1} for 15^1 are well reproduced by the B3LYP calculation with 439 and 64 cm^{-1}. The BP86 calculation predicts the 15^1 correctly with 67 cm^{-1}, while it slightly overestimates the 6b^1 with 463 cm^{-1}. The CC2 calculation gives good results in predicting the 6b^1 with 439 cm^{-1}, while it overestimates the 15^1 with 154 cm^{-1}.

4.2.2. MATI spectra. The MATI spectra *via* the S_1 intermediate states 0^0, 17b^1, 9a^1 are shown in Fig. 4. The origin of the $D_0(^2B_1)$ state and with that the adiabatic ionization energy was found to be 75.627 ± 6 cm^{-1} (9.3765 ± 0.0007 eV). This value is in good accordance the previously by photoelectron spectroscopy determined value of 9.37 ± 0.02 eV.[25]

In accordance with the $\Delta v = 0$ propensity rule, the MATI spectrum obtained *via* the electronic origin is dominated by the 0^0-band. Furthermore the spectrum is characterized by strong activity of the two total symmetric modes 9a^1 and 6a^1. Within the recorded range of 1000 cm^{-1}, the spectrum exhibits a progression in 9a composed of the first three overtones 9a^1 (293 cm^{-1}), 9a^2 (588 cm^{-1}) and 9a^3 (882 cm^{-1}). The 6a appears as ground vibration 6a^1 (418 cm^{-1}), first overtone 6a^2 (839 cm^{-1}) as well as combination vibration 9a^{1}6a^1 (706 cm^{-1}).

Additionally we assigned the band at 925 cm^{-1} to a combination band of modes 9a^{1}1^1. The relative intensive band at 630 cm^{-1} has been identified with the mode 1^1. The shoulder at 649 cm^{-1} in the peak labeled with 1^1 has been assigned to the mode 4^1. Exhibiting a similar weak intensity as the 4^1, another b_1-symmetrical mode (7a^1) could be identified at 778 cm^{-1}. In the view of previous work,[1] the assignment of the bands at 95 cm^{-1}

Table 2 Comparison experimental and calculated normal modes observed in the S_0, S_1 and D_0 state of 1,3,2 DFCB

$S_0(C_{2v})$						S_1	(C_{2v})	(C_{2v})	(C_S)	D_0	(C_{2v})	
Wilson	Sym.	exp.	B3LYP	BP86	CC2	exp.	B3LYP	BP86	CC2	exp.	B3LYP	BP86
9a	a_1		301	290	295	228	374	364	367	293	304	294
6a	a_1		437	425	436	381	198	202	188	418	435	422
1	a_1		617	602	618	607	517	500	488	630	636	620
7a	a_1		783	760	776		748	729	713	778	784	761
19a	a_1		1072	1142	1124		1506	1462	1360		1360	1318
18a	a_1		1121	1042	1065		1113	1083	1059		1045	1021
12	a_1		1314	1275	1317		1005	984	949		1150	1114
13	a_1		1494	1448	1491		1294	1252	1268		1413	1372
8a	a_1		1637	1587	1635		1577	1542	1507		1665	1613
20a	a_1		3191	3121	3224		3201	3133	3212		3199	3128
2	a_1		3212	3143	3248		3223	3155	3266		3217	3148
10a	a_2		249	239	247		194	189	183	201	218	209
16a	a_2		597	573	588		762	766	519	546	565	541
17a	a_2		893	850	873		1043	1107	788		920	880
17b	b_1		124	119	125	25	31	41	51	97	98	94
10b	b_1		275	264	273	198	215	214	176	280	289	277
16b	b_1		530	510	521	404	428	407	351	439	434	415
4	b_1		717	684	675		805	779	649	649	729	700
11	b_1		792	754	772		640	632	548	839	837	802
5	b_1		968	922	944		979	946	781		1000	954
15	b_2		212	204	208	63	64	67	154	213	221	212
6b	b_2		509	494	501	443	451	463	439	367	386	369
3	b_2		555	534	543		511	501	492	489	539	522
7b	b_2		1020	990	1014		979	958	948	982	1018	986
9b	b_2		1179	1088	1167		1137	1128	1133		1110	1087
18b	b_2		1266	1226	1262		1208	1171	1194		1303	1259
14	b_2		1322	1331	1424		1380	1393	1456		1354	1316
19b	b_2		1503	1456	1495		1441	1382	1381		1548	1500
8b	b_2		1626	1577	1623		1477	1451	1680		1381	1370
20b	b_2		3206	3137	3242		3207	3139	3215		3214	3145

Table 3 B3LYP/TZVPP calculated geometries of 1,3,2-DCFB

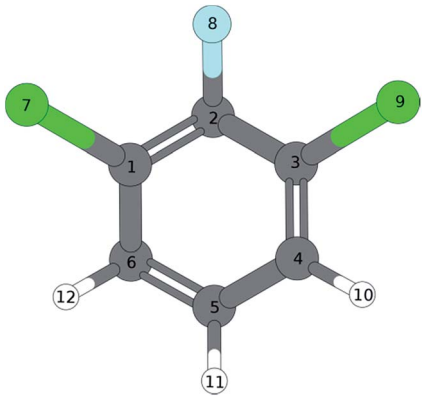

B3LYP/TZVPP	C_{2v}	C_2	C_{2v}
Bond length [Å]	S_0	S_1	D_0
C1–C2	1.391	1.364	1.438
C2–C3	1.391	1.445	1.438
C3–C4	1.389	1.403	1.373
C4–C5	1.389	1.370	1.407
C5–C6	1.389	1.370	1.407
C6–C1	1.389	1.380	1.373
C1–Cl7	1.739	2.358	1.698
C2–F8	1.334	1.325	1.290
C3–Cl9	1.739	1.700	1.698
C4–H10	1.080	1.080	1.081
C5–H11	1.081	1.082	1.082
C6–H12	1.080	1.085	1.081
Bond angles [°]			
C1–C2–C3	120.125	123.523	122.001
C2–C3–C4	119.972	119.825	118.077
C3–C4–C5	119.648	117.525	119.488
C4–C5–C6	120.635	120.436	122.869
C5–C6–C1	119.648	123.643	119.488
C6–C1–C2	119.972	115.049	118.077
Cl7–C1–C2	119.336	131.346	118.378
C1–C2–F8	119.938	121.023	118.996
C4–C3–Cl9	120.692	120.051	123.541
Dihedral angle [°]			
Cl7–C1–C6–H12	0	−0.018	0
Cl7–C1–C2–F8	0	0.016	0
Cl9–C3–C4–H10	0	−0.005	0

Table 4 BP86/TZVPP calculated geometries of 1,3,2-DCFB

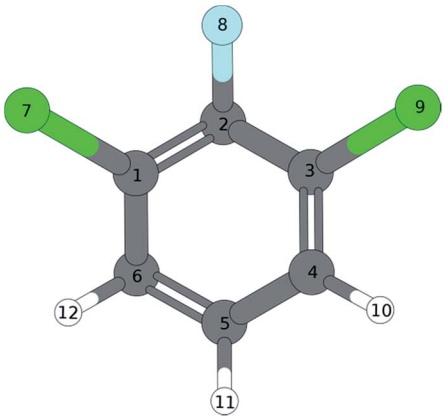

BP86/TZVPP	C_{2v}	C_2	C_{2v}
Bond length [Å]	S_0	S_1	D_0
C1–C2	1.400	1.377	1.444
C2–C3	1.400	1.445	1.444
C3–C4	1.396	1.411	1.382
C4–C5	1.395	1.379	1.411
C5–C6	1.395	1.434	1.411
C6–C1	1.396	1.395	1.382
C1–Cl7	1.740	2.325	1.701
C2–F8	1.341	1.335	1.300
C3–Cl9	1.740	1.708	1.701
C4–H10	1.088	1.088	1.089
C5–H11	1.089	1.090	1.090
C6–H12	1.088	1.094	1.089
Bond angles [°]			
C1–C2–C3	120.007	123.861	121.791
C2–C3–C4	120.019	120.100	118.195
C3–C4–C5	119.613	117.257	119.447
C4–C5–C6	120.728	120.361	122.865
C5–C6–C1	119.613	124.461	119.477
C6–C1–C2	120.019	113.959	118.195
Cl7–C1–C2	119.198	130.690	118.269
C1–C2–F8	119.938	121.023	118.996
C4–C3–Cl9	120.783	119.621	123.535
Dihedral angle [°]			
Cl7–C1–C6–H12	0	−0.030	0
Cl7–C1–C2–F8	0	0.038	0
Cl9–C3–C4–H10	0	−0.006	0

and 196 cm^{-1} to the modes $17b^1$ and $17b^2$ respectively seems appropriate. Assignments that are more tentative are the $16b^1$ and 11^1 to the bands at 439 cm^{-1} and 839 cm^{-1}. The a_2-symmetrical modes $10a^1$ and $16a^1$ are assigned to the weak bands at 201 cm^{-1} and 546 cm^{-1}. With exception of 4^1 all calculated frequencies are in good accordance with the experimentally determined ones.

Provided the validity of the $\Delta v = 0$ propensity rule, the MATI spectrum obtained *via* the $S_1 17b^1$ mode ought to be characterized by a towering $17b^1$ band. Contrary to expectations, the band $17b^1$ could not be observed in the spectrum shown in Fig. 4. Instead, the spectrum shows the $9a^1$ at 291 cm^{-1} as the most intensive resonance absorption. As can be seen from the correlation between the MATI spectra in Fig. 4, the first overtone $9a^2$ appears at 586 cm^{-1} as well. The signals at 419 cm^{-1} and 629 cm^{-1} are identified as the $6a^1$ and 1^1 total symmetric modes. Obviously, the signals for the 11-vibration is broadened. Based on the MATI spectrum of the 0^0 transition, we assigned this signal both to the 1^1 and 4^1 vibrations, the latter of which gives rise to the shoulder. The MATI spectrum obtained *via* the $S_1 9a^1$ shows three prominent peaks: the $6a^1$, the $9a^1 6a^1$ and the $18a^1$. Without folding the spectrum with the laser

Table 5 CC2/cc-pVTZ calculated geometries of 1,3,2-DCFB

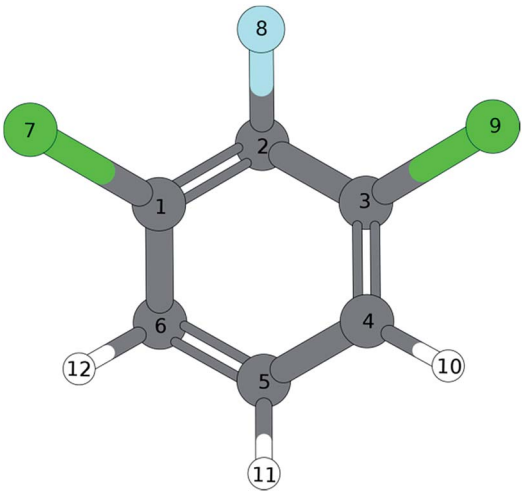

BP86/TZVPP	C_{2v}	C_2
Bond length [Å]	S_0	S_1
C1–C2	1.395	1.432
C2–C3	1.395	1.432
C3–C4	1.393	1.426
C4–C5	1.393	1.421
C5–C6	1.393	1.421
C6–C1	1.393	1.426
C1–Cl7	1.725	1.719
C2–F8	1.333	1.326
C3–Cl9	1.725	1.719
C4–H10	1.080	1.079
C5–H11	1.081	1.082
C6–H12	1.080	1.079
Bond angles [°]		
C1–C2–C3	119.992	121.970
C2–C3–C4	120.078	118.706
C3–C4–C5	119.618	118.910
C4–C5–C6	120.617	122.532
C5–C6–C1	119.618	118.910
C6–C1–C2	120.078	118.706
Cl7–C1–C2	119.105	118.817
C1–C2–F8	120.004	119.015
C4–C3–Cl9	110.817	120.760
Dihedral angle [°]		
Cl7–C1–C6–H12	0	−17.842
Cl7–C1–C2–F8	0	17.222
Cl9–C3–C4–H10	0	−17.842

Table 6 B3LYP/TZVPP calculated geometries of 1,3,2-DFCB

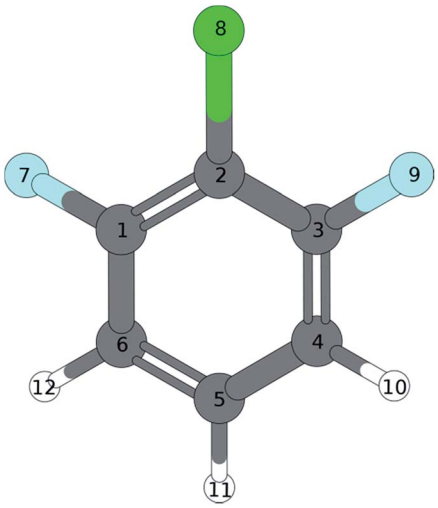

B3LYP/TZVPP	C_{2v}	C_{2v}	C_{2v}
Bond length [Å]	S_0	S_1	D_0
C1–C2	1.393	1.365	1.440
C2–C3	1.393	1.365	1.440
C3–C4	1.384	1.444	1.365
C4–C5	1.389	1.384	1.409
C5–C6	1.389	1.384	1.409
C6–C1	1.384	1.444	1.365
C1–F7	1.340	1.326	1.309
C2–Cl8	1.729	2.361	1.665
C3–F9	1.340	1.326	1.309
C4–H10	1.081	1.081	1.081
C5–H11	1.081	1.080	1.082
C6–H12	1.081	1.081	1.081
Bond angles [°]			
C1–C2–C3	117.528	111.693	118.393
C2–C3–C4	121.919	126.328	120.838
C3–C4–C5	118.997	118.962	118.528
C4–C5–C6	120.640	117.726	122.876
C5–C6–C1	118.997	118.962	118.528
C6–C1–C2	117.528	126.328	120.838
F7–C1–C2	118.843	120.164	117.338
C1–C2–Cl8	121.236	124.155	120.803
C4–C3–F9	119.237	113.508	121.823
Dihedral angle [°]			
F7–C1–C6–H12	0	0.027	0
F7–C1–C2–Cl8	0	−0.204	0
F9–C3–C4–H10	0	−0.032	0

power, no absolute statement can be made in regards to the peak intensities. The three peaks are of nearly equal intensity (approx. 5% difference), so it is hard to tell which one is the highest in intensity. Nevertheless it can be stated that in contrary to the predictions of the propensity rule, transitions to $6a^1$ and $9a^16a^1$ are at least as same as intensive while the vertical transition into the D_09a^1 state is scarcely visible in the spectrum. Nevertheless the mode 9a appears in a series of overtones $9a^16a^1$ (710 cm^{-1}), $9a^11^1$ (924 cm^{-1}) and $9a^26a^1$ (1003 cm^{-1}). Remarkably, the spectrum exhibits a strong activity in 6a modes: the bands assigned to the modes $6a^1$ and $9a^16a^1$ are among the three most intense bands in the spectrum. The $6a^1$ vibration shows progression activity ($6a^1$ and $6a^2$ in the recorded range). In addition, the $6a^1$ mode contributes to overtone bands as already discussed above. The weak features at 97, 193 and 213 cm^{-1} have been assigned on the basis of our previous

Table 7 BP86/TZVPP calculated geometries of 1,2,3-DFCB

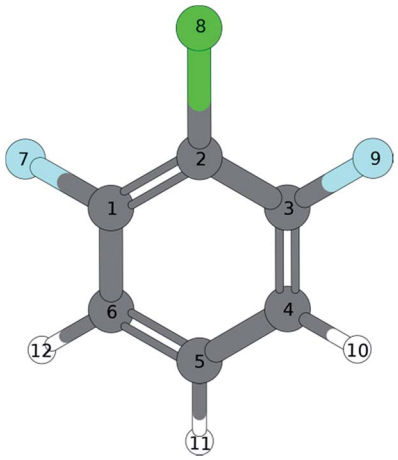

BP86/TZVPP	C_{2v}	C_{2v}	C_{2v}
Bond length [Å]	S_0	S_1	D_0
C1–C2	1.401	1.378	1.446
C2–C3	1.401	1.378	1.446
C3–C4	1.391	1.446	1.374
C4–C5	1.396	1.391	1.414
C5–C6	1.396	1.391	1.414
C6–C1	1.391	1.446	1.374
C1–F7	1.348	1.337	1.318
C2–Cl8	1.730	2.332	1.671
C3–F9	1.348	1.337	1.318
C4–H10	1.089	1.089	1.089
C5–H11	1.089	1.087	1.090
C6–H12	1.089	1.089	1.089
Bond angles [°]			
C1–C2–C3	117.514	110.326	118.508
C2–C3–C4	121.885	127.177	120.727
C3–C4–C5	118.999	118.870	118.543
C4–C5–C6	120.718	117.579	122.956
C5–C6–C1	118.999	118.870	118.543
C6–C1–C2	117.514	127.177	120.727
F7–C1–C2	118.763	119.276	117.392
C1–C2–Cl8	121.242	124.836	120.740
C4–C3–F9	119.349	113.548	121.870
Dihedral angle [°]			
F7–C1–C6–H12	0	0.041	0
F7–C1–C2–Cl8	0	−0.191	0
F9–C3–C4–H10	0	−0.032	0

Table 8 CC2/cc-pVTZ calculated geometries of 1,2,3-DFCB

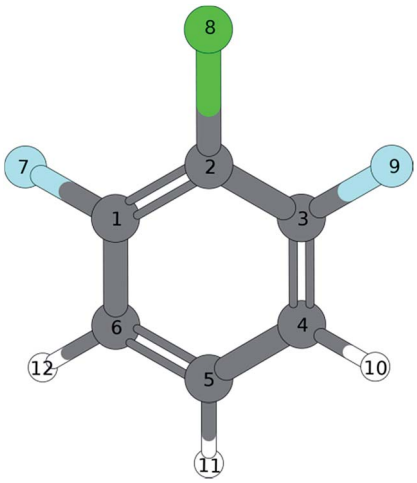

B3LYP/TZVPP	C_{2v}	C_{2v}
Bond length [Å]	S_0	S_1
C1–C2	1.396	1.416
C2–C3	1.396	1.416
C3–C4	1.387	1.431
C4–C5	1.394	1.407
C5–C6	1.394	1.407
C6–C1	1.387	1.431
C1–F7	1.339	1.337
C2–Cl8	1.716	1.825
C3–F9	1.339	1.337
C4–H10	1.080	1.825
C5–H11	1.081	1.337
C6–H12	1.080	1.083
Bond angles [°]		
C1–C2–C3	117.753	110.391
C2–C3–C4	121.786	125.833
C3–C4–C5	118.972	120.624
C4–C5–C6	120.732	116.095
C5–C6–C1	118.972	120.624
C6–C1–C2	121.786	125.833
F7–C1–C2	118.680	118.508
C1–C2–Cl8	121.124	118.556
C4–C3–F9	119.534	115.651
Dihedral angle [°]		
F7–C1–C6–H12	0	0.912
F7–C1–C2–Cl8	0	46.945
F9–C3–C4–H10	0	−0.912

studies[7,8] to the out-of-plane modes $17b^1$, $17b^2$ and in-plane mode 15^1.

5. Discussion

5.1. 1,3,2-DCFB

Compared to electronic and cationic ground states the 17b exhibits a drastically decreased frequency in the first electronic excited state (see Table 1). Such a frequency lowering suggests a geometrical distortion along the eigenvector of 17b in going from S_0 to S_1 or from D_0 to S_1, respectively. As considered earlier by Tsuchiya *et al.*[14] for difluorobenzene it is highly suggested that this phenomenon is the result of strong vibronic coupling between the S_1 and nearby states. But the most important indication for a such a distortion shows up in the MATI spectra *via* the electronic origin and, first and foremost, *via* the $17b^2$. The latter exhibits a three-membered progression of the mode 17b. Not just that this progression shows a shift of the Franck–Condon maximum between S_1 and D_0, the fact that the transition from $D_0 17b^1 \leftarrow S_1 17b^2$ is favored could be interpreted as a

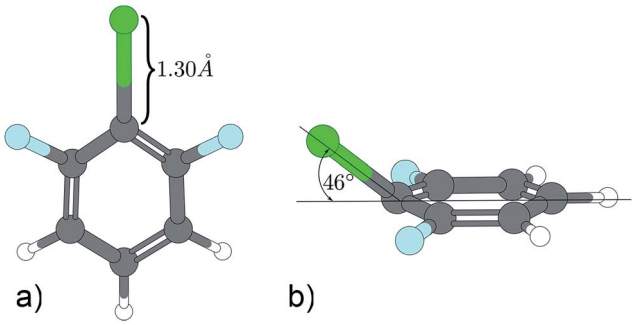

Fig. 6 Excited state geometry of 1,3,2-DFCB obtained by different quantum mechanical methods. (a) TDDFT, (b) CC2.

replanarisation of the molecular geometry in going from S_1 to D_0 along that mode.

Also during ionization *via* the vibrationless level of the first excited state, the transition $D_0 17b^1 \leftarrow S0^0$ is clearly favored over $D_0 0^0 \leftarrow S_1 0^0$ (see MATI *via* 0^0 Fig. 2). A major role of the 17b mode during ionization is aggravated by the fact the 17b also appears as combination bands ($17b^1 9a^1$ in each of the recorded MATI spectra, $17b^1 6b^1$ in the MATI *via* $17b^2$). The strong activity of the mode $16b^1$ in the MATI *via* $17b^2$ and the general, unusual appearance of multiple other out-of-plane modes throughout the MATI spectra give rise to the assumption that the geometry in the S_1 is a product of a distortion along several modes. The CC2 computed geometry optimization seem to support the statements derived from the experimental data: the geometry shown in Fig. 5 is obviously not just the product of a distortion along a single (out-of-plane) normal mode (Table 2).

The quantum chemical calculations predict a $S_1(\pi^* \leftarrow \pi)$ transition into the first excited state for 1,3,2-DCFB. However, due to σ*-orbitals localized on the Halogen–Carbon bond, it is possible for modes of appropriate symmetry to induce coupling to (πσ*)-states. In accordance with the assumption of a vibronic coupling effect we prevalently observed a substantial decrease in frequency comparing the S_0 state and the S_1 state of the neutral for formal forbidden modes with strong influence of halogen atoms on their displacement pattern. For the modes 15, 6b, 3 (b_2 symmetry) and 16a (a_2 symmetry) we observed such a decrease.

The decrease in frequency for the modes 15, 6b, 3 is explainable in accordance with the Herzberg–Teller (HT) effect. However, the frequency lowering of the symmetry allowed mode $17b^2$ could not be described in terms of the HT effect in a sufficient way. It seems that the distortion along 17b blurs the symmetry differences between the (πσ*)- and (ππ*)-states which would be an indication for a pseudo Jahn–Teller effect.

5.2. 1,3,2-DFCB

In 1,3,2-DFCB the vibration 15 appears in the REMPI spectrum as a progression-forming and largely frequency lowered mode. Remarkably, the progression reveals a negative anharmonicity. The occurrence of the 15 as a b_2 symmetric mode is explained in terms of the Herzberg–Teller effect. Besides the mode 15, also the modes 6a and 9a exhibit a largely lowered frequency in the first excited state S_1. Both modes are likely to contribute in pseudo Jahn–Teller distortion in going from the electronic ground to excited state or from excited state to ionic ground state, respectively. This is seen from the different MATI spectra as well as the different calculated structures given in Tables 3–8. The MATI spectrum *via* the electronic origin exhibits a harmonic, three-membered progression of mode 9a ($9a^1$, $9a^2$, $9a^3$), whereby the band $9a^1$ is almost as intense as the 0–0 transition. Such a shift of the Franck–Condon maximum is a clear indication for a distortion along the eigenvector of this mode during ionization.

A similar situation is found in the MATI spectrum *via* $9a^1$. Here, in contradiction to the $\Delta v = 0$ propensity rule, the transition into the $S_1 6a^1$ state is the most favorable while the vertical transition into the $9a^1$ is scarcely observable. Nevertheless the mode 9a is strongly present in overtones ($9a^1 6a^1$, $9a^1 1^1$, $9a^2 6a^1$). The geometry found by the TDDFT calculations (Fig. 6a; Tables 6 and 7) support the experimental findings in predicting a C_{2v}-symmetric structure distorted along the 6a. The CC2 calculation suggests a 17b-like distorted structure (Fig. 6b; Table 8).

The CC2 calculation suggests a 17b-like distorted structure (Fig. 6b). Considering the vanishing low activity of 17b in the MATI spectra, the suggestion seems incorrect. Nevertheless the substantial decrease in frequency for $6a^1$ and $9a^1$ comparing the D_0 state and the S_1 state is accurately reproduced by all quantum chemical methods employed. Comparing experimental and calculated results for 1,3,2-DFCB, the unusual, striking deviation (up to 49%) for a_1-symmetrical S_1-frequencies was particularly noticeable. A poor reproduction of the molecular equilibrium structure in the S_1 (wrong minimum on the PES) could be one possible explanation.

A contrary indication is the fact that we find very similar frequencies for widely differing structures predicted by TDDFT (planar structure) and CC2 method (out-of-plane-structure). The planar structure resembles the experimental observations well, but since all frequency analyses were performed in harmonic approximation, a strong anharmonicity for this particular vibrations could be another explanation for this findings.

6. Conclusion

Comparing the results from two compounds presented in this paper with results obtained from different isomeric trichlorobenzenes,[1] the increasing number of fluorine atoms lead to a progressive decrease in some of the observed frequencies in going from S_0 to S_1 and from D_0 to S_1, respectively. This is especially true for modes with a strong fluorine participation in their vibrational pattern like 17b (*cf.* Table 1). We interpreted this as a strong indication for an out-of-plane distortion during excitation or a replanarisation during ionization along the eigenvector of those modes. This phenomenon could be attributed to an above, bounding S(πσ*) state which is stabilized by an increasing number of fluorine atoms.[12] It can be concluded that the fluorine atoms contribute a significant share in form of $\sigma^* \leftarrow \pi$ character to the transition.

For 1,3,2-DCFB the quantum chemical calculations gave excitation energies (EE) of 5.06 eV (B3LYP/TZVPP), 4.71 eV

(BP86/TZVPP) and 4.44 eV (CC2/cc-pVTZ). The CC2 value reproduces the experimental value of 4.52 eV with a deviation of 0.08 eV best.

The experimental value for the ionization energy (IE) of 9.32 eV is underestimated by both DFT methods with 9.00 eV (B3LYP/TZVPP) and 8.97 eV (BP86/TZVPP). (The coupled cluster method CC2 is not suited for the ionic species!). In this case the frequency analysis performed by the CC2 method showed to be most appropriate to reproduce the experimental frequencies.

For 1,3,2-DFCB the quantum chemical calculations gave excitation energies (EE) of 5.23 eV (B3LYP/TZVPP), 4.90 eV (BP86/TZVPP) and 3.88 eV (CC2/cc-pVTZ). The TDDFT value reproduces the experimental value of 4.64 eV best, whereas BP86 underestimates and B3LYP overestimates the experimental value. Both DFT methods with 9.03 eV (B3LYP/TZVPP) and 9.02 eV (BP86/TZVPP) underestimate the experimental value for the ionization energy (IE) of 9.38 eV. Contrary to the 1,3,2 DCFB the frequency analysis performed by the DFT methods results in a better reproduction of the experimental frequencies for the 1,3,2 DFCB.

Furthermore the $S_1 \leftarrow S_0$ electronic excitation energies (EE) and $D_0 \leftarrow S_0$ adiabatic ionization energies (IE) could be determined very exactly:

EE(1,3,2-DFCB) = 36 460 ± 2 cm^{-1}, IE(1,3,2-DFCB) = 75.242 ± 6 cm^{-1};

EE(1,3,2-DCFB) = 37 449 ± 2 cm^{-1}, IE(1,3,2-DCFB) = 75.627 ± 6 cm^{-1}.

References

1 F. Witte, R. Mikko, F. Gunzer and J. Grotemeyer, Mass analyzed threshold ionization (mati) spectroscopy of trichlorobenzenes via different intermediate vibrational states in the s1 state, *Int. J. Mass Spectrom.*, 2011, **306**, 129–137, DOI: 10.1016/j.ijms.2010.10.002.

2 L. Yuan, C. Li, J. Lin, S. Yang and W. Tzeng, Mass analyzed threshold ionization spectroscopy of o-fluorophenol and o-methoxyphenol cations and influence of the nature and relative location of substituents, *Chem. Phys.*, 2006, **323**, 429–438, DOI: 10.1016/j.chemphys.2005.10.004.

3 K. Müller-Dethlefs, M. Sander and E. W. Schlag, Two-colour photoionization resonance spectroscopy of NO: complete separation of rotational levels of NO^+ at the ionization threshold, *Chem. Phys. Lett.*, 1984, **112**, 291–294, DOI: 10.1016/0009-2614(84)85743-7.

4 L. Zhu and P. Johnson, Mass analyzed threshold ionization spectroscopy, *J. Chem. Phys.*, 1991, **94**(8), 5769–5771, DOI: 10.1063/1.460460.

5 K. Walter, U. Boesl and E. W. Schlag, Molecular ion spectroscopy: resonance-enhanced multiphoton dissociation spectra of the fluorobenzene cation, *Chem. Phys. Lett.*, 1989, **162**(4, 5), 261–268, DOI: 10.1016/0009-2614(89)87041-1.

6 G. Reiser, D. Rieger, T. G. Wright, K. Müller-Dethlefs and E. W. Schlag, Zero-kinetic-energy (ZEKE) photoelectron spectroscopy of p-difluorobenzene via different intermediate vibrational levels in the s1 state, *J. Phys. Chem.*, 1993, **97**, 4335–4343, DOI: 10.1021/j100119a015.

7 A. Gaber, M. Riese and J. Grotemeyer, Mass analyzed threshold ionization spectroscopy of o-, m-, and p-dichlorobenzenes. Influence of the chlorine position on vibrational spectra and ionization energy, *J. Phys. Chem. A*, 2008, **112**, 425–434, DOI: 10.1021/jp074802t.

8 A. Gaber, M. Riese and J. Grotemeyer, Detailed analysis of the cation ground state of three dichlorobenzenes by mass analyzed threshold ionization spectroscopy, *Phys. Chem. Chem. Phys.*, 2008, **10**, 1168–1176, DOI: 10.1039/B715496H.

9 C. Weickhardt, R. Zimmermann, K. W. Schramm, U. Boesl and E. W. Schlag, Laser mass spectrometry of the di-, tri- and tetrachlorobenzenes: isomer-selective ionization and detection, *Rapid Commun. Mass Spectrom.*, 1994, **8**, 381–384, DOI: 10.1002/rcm.1290080508.

10 C. H. Kwon and M. S. Kim, One-photon mass-analyzed threshold ionization spectroscopy of 1,3,5-trifluorobenzene: the Jahn–Teller effect and vibrational analysis for the molecular cation in the ground electronic state, *J. Chem. Phys.*, 2004, **121**(6), 2622–2629, DOI: 10.1063/1.1765655.

11 S. Sato, K. Ikeda and K. Kimura, Zeke photo electron spectroscopy and ab initio force-field calculation of 1,2,4,5-tetrafluorobenzene, *J. Electron. Spectrosc. Relat. Phenom.*, 1998, **88–91**, 137–142, DOI: 10.1016/S0368-2048(97)00256-9.

12 M. Z. Zgierski, T. Fujiwara and E. C. Lim, Photophysics of aromatic molecules with low-lying pi sigma * states: fluorinated benzenes, *J. Chem. Phys.*, 2005, **122**(14), 144312, DOI: 10.1063/1.1873752.

13 C. H. Kwon and M. S. Kim, Vacuum ultraviolet mass-analyzed threshold ionization spectroscopy of hexafluorobenzene: the Jahn–Teller effect and vibrational analysis, *J. Chem. Phys.*, 2004, **120**(24), 11578, DOI: 10.1063/1.1753258.

14 Y. Tsuchiya, K. Takazawa, M. Fujii and M. Ito, Electronic spectra of o-, m-, p-difluorobenzene cations: striking similarity in vibronic coupling between the neutral molecule and its cation, *J. Phys. Chem.*, 1992, **96**(1), 99–104, DOI: 10.1021/j100180a022.

15 F. Gunzer and J. Grotemeyer, New features in the mass analysed threshold ionization (MATI) spectra of alkyl benzenes, *Phys. Chem. Chem. Phys.*, 2002, **24**, 5966–5972, DOI: 10.1039/b208283g.

16 F. Gunzer and J. Grotemeyer, Enhancing of the signal-to-noise ratio in MATI spectra, *Int. J. Mass Spectrom.*, 2003, **228**, 921–931, DOI: 10.1016/S1387-3806(03)00195-7.

17 R. Ahlrichs, M. Bär, M. Häser, H. Horn and C. Kölmel, Electronic structure calculations on workstation computers: the program system turbomole, *Chem. Phys. Lett.*, 1989, **162**, 165–169, DOI: 10.1016/0009-2614(89)85118-8.

18 M. v. Arnim and R. Ahlrichs, Geometry optimization in generalized natural internal coordinates, *J. Chem. Phys.*, 1999, **111**, 9183–9190, DOI: 10.1063/1.479510.

19 M. Häser and R. Ahlrichs, Improvements on the direct SCF method, *J. Comput. Chem.*, 1989, **10**, 104–111, DOI: 10.1002/jcc.540100111.

20 O. Treutler and R. Ahlrichs, Efficient molecular numerical integration schemes, *J. Chem. Phys.*, 1995, **102**, 346–354, DOI: 10.1063/1.469408.

21 (*a*) A. D. Becke, Density functional calculations of molecular bond energies, *J. Chem. Phys.*, 1986, **84**, 4524–4529, DOI: 10.1063/1.450025; (*b*) A. Becke, Density-functional exchange-energy approximation with correct asymptotic behavior, *Phys. Rev. A: At., Mol., Opt. Phys.*, 1988, **38**, 3098, DOI: 10.1103/PhysRevA.38.3098; (*c*) F. Weigend, M. Häuser, H. Patzelt and R. Ahlrichs, RI-MP2: optimized auxiliary basis sets and demonstration of efficiency, *Chem. Phys. Lett.*, 1998, **294**, 143–152, DOI: 10.1016/S0009-2614(98)00862-8; (*d*) F. Weigend, A. Köhn and C. Hättig, Efficient use of the correlation consistent basis sets in resolution of the identity MP2 calculations, *J. Chem. Phys.*, 2002, **116**, 3175–3183, DOI: 10.1063/1.1445115.

22 G. Varsanyi and S. Szoke, *Vibrational Spectra of Benzene Derivatives*, Academic Press, New York, London, 1969.

23 E. B. Wilson, The normal modes and frequencies of vibration of the regular plane hexagon model of the benzene molecule, *J. Phys. Rev.*, 1934, **41**, 706–714, DOI: 10.1103/PhysRev.45.706.

24 J. Green, D. Harrison and W. Kynaston, Vibrational spectra of benzene derivatives-XI 1,3,5- and 1,2,3-trisubstituted compounds, *Spectrochim. Acta, Part A*, 1971, **27**(6), 793–806, DOI: 10.1016/0584-8539(71)80158-7.

25 M. Mohraz, J. Maier and E. Heilbronner, He(Iα) and He(IIα) photoelectron spectra of fluorinated chloro- and bromobenzenes, *J. Electron Spectrosc. Relat. Phenom.*, 1980, **19**, 429–446, DOI: 10.1016/0368-2048(80)80063-6.